Journal of Sound and Vibration (1998) **214**(1), 183–194

LETTERS TO THE EDITOR

PERIODIC RESPONSE AND BIFURCATIONS OF AN SDF SYSTEM WITH ORIFICE DAMPING

A. Raghothama and S. Narayanan

Machine Dynamics Laboratory, Department of Applied Mechanics, Indian Institute of Technology, Madras, Chennai 600 036, *India*

(*Received* 13 *November* 1996, *and in final form* 13 *May* 1997)

1. INTRODUCTION

The vibratory behaviour of systems with non-linear damping characteristics such as piecewise linear, dry friction, quadratic and cubic damping with applications to different mechanical vibrating systems has been analysed both numerically and analytically. Such systems find applications as practical vibration isolation devices as in pneumatic suspensions and wire rope vibration isolators. Ravindra and Mallik [1] have analysed a non-linear vibration isolation device with cubic stiffness and quadratic damping and have reported chaotic behaviour of the same through period doubling and intermittency routes. An orifice type of damping is present in shock absorbers as in aircraft oleo-pneumatic landing gears. In this paper, the periodic motions and bifurcational behaviour of a non-linear system with cubic stiffness and orifice type damping subjected to a harmonic excitation are analysed using the incremental harmonic balancing (IHB) procedure.

The IHB method [2] is a numeric-analytic technique which is extended here in a general form to consider different types of damping non-linearities such as cubic, piecewise linear, quadratic, dry friction and orifice damping. Leung and Fung [3] have used the IHB method to obtain regions of chaos in the parametric space for Duffing's oscillator. The IHB formulations were extended to analyse the periodic vibrations of systems with piecewise linear stiffness characteristics by Lau and Zhang [4]. Pierre *et al*. [5] have applied the IHB method to analyse the steady state motions of systems with dry friction.

The bifurcation study is facilitated by coupling the IHB method with a stability analysis of the periodic motions. A path following algorithm using arc-length extrapolation as given by Leung and Chui [6] is adopted giving further insight into the bifurcational behaviour.

2. PROBLEM FORMULATION

The equation of motion of a single-degree-of-freedom (sdf) non-linear system with pth power damping and cubic stiffness can be expressed in non-dimensional form as

$$\ddot{x} + 2\xi\dot{x}|\dot{x}|^{p-1} + x^3 = F\cos\Omega\tau, \qquad \xi > 0, \qquad p > 0, \tag{1}$$

where x is the non-dimensional displacement, Ω is the non-dimensional frequency and overdots represent order of differentiation with respect to non-dimensional time τ.

The values of exponent $p = 0$, 1, 1·5, 2, 3, correspond respectively to Coulomb, linear, orifice, quadratic and cubic damping. The parameters ξ and F in equation (1) refer respectively to the extent of damping and amplitude of the exciting force. For orifice damping equation (1) reduces to

$$\ddot{x} + 2\xi H(\dot{x})\dot{x}^{3/2} + x^3 = F\cos\Omega\tau, \qquad \xi > 0, \qquad p > 0, \tag{2}$$

0022–460X/98/260183 + 12 $25.00/0/sv971553

where H is the Heaveside unit step function. For the purpose of obtaining the periodic solutions of equation (2) by the IHB method, it is convenient to express $\dot{x}^{3/2}$ in terms of the least square polynomial as

$$\dot{x}^{3/2} = -\frac{8}{33W^{3/2}}\dot{x}^3 + \frac{72}{77W^{1/2}}\dot{x}^2 + \frac{24}{77}W^{1/2}\dot{x} - \frac{8}{1155}W^{3/2}, \tag{3}$$

where W is the maximum value of $\dot{x}$ within a period.

3. IHB METHOD FOR PIECEWISE NON-LINEAR DAMPED SYSTEM

3.1. *General formulation*

Consider a non-linear system in the general form

$$g(\ddot{x}, \dot{x}, x, F, \Omega, \tau) = 0. \tag{4}$$

The first step in applying the IHB method to obtain the periodic solutions is to increment from some initial guess of the solution of equation (4), x_0, F_0, Ω_0, to the actual solution x^*, F^*, Ω^* iteratively. Using a Taylor series expansion, one gets

$$\begin{aligned} &g(x_0 + \Delta x, \dot{x}_0 + \Delta\dot{x}, \ddot{x}_0 + \Delta\ddot{x}, F_0 + \Delta F, \Omega_0 + \Delta\Omega, \tau) \\ &= g_0 + \frac{\partial g}{\partial x}\bigg|_0 \Delta x + \frac{\partial g}{\partial \dot{x}}\bigg|_0 \Delta\dot{x} + \frac{\partial g}{\partial \ddot{x}}\bigg|_0 \Delta\ddot{x} + \frac{\partial g}{\partial F}\bigg|_0 \Delta F + \frac{\partial g}{\partial \Omega}\bigg|_0 \Delta\Omega \\ &\quad + \text{higher order terms} = 0. \end{aligned} \tag{5}$$

The subscript 0 represents the evaluation of the relevant quantities corresponding to x_0, $\dot{x}_0$ etc. For obtaining periodic solutions of the original equation of motion, the higher order terms are neglected and x and Δx are expanded in a finite Fourier series in the form

$$x(\tau) = a_0 + \sum_{i=1}^{N} (a_i \cos i\tau + b_i \sin i\tau),$$

$$\Delta x = \Delta a_0 + \sum_{i=1}^{N} (\Delta a_i \cos i\tau + \Delta b_i \sin i\tau). \tag{6}$$

For the approximate solution assumed in equation (6) to converge to the actual solution, a Galerkin procedure is adopted to minimize the equation error $\varepsilon(\tau)$ which is given by the terms on the right side of equation (5), excluding the higher order terms. The minimization results in the orthogonalizing relations.

$$\int_0^{2\pi} \varepsilon(\tau) \begin{Bmatrix} \cos i\tau \\ \sin i\tau \end{Bmatrix} \mathrm{d}\tau = 0. \tag{7}$$

This represents a set of $2N$ matrix algebraic linear equations of the form

$$\{\mathbf{R}\} = [\mathbf{C}]\Delta a + \{\mathbf{P}\}\Delta F + \{\mathbf{Q}\}\Delta\Omega, \tag{8}$$

where $[\mathbf{C}]$ is the Jacobian matrix corresponding to response, $\{\mathbf{R}\}$ is the residual vector, $\{\mathbf{\Delta a}\}$ the incremental vector in the Fourier cosine and sine coefficients and $\{\mathbf{P}\}$, $\{\mathbf{Q}\}$ refer to the

derivative vector corresponding to F and Ω, respectively. These elements are defined in the form

$$\{\mathbf{R}\} = \begin{Bmatrix} R_{ai} \\ R_{bi} \end{Bmatrix}, \quad [\mathbf{C}] = \begin{bmatrix} K_{ij}^{cc} & K_{ij}^{cs} \\ K_{ij}^{sc} & K_{ij}^{ss} \end{bmatrix}, \quad \{\mathbf{\Delta a}\} = \begin{Bmatrix} \Delta a_i \\ \Delta b_i \end{Bmatrix}, \quad \{\mathbf{P}\} = \begin{Bmatrix} P_{ai} \\ P_{bi} \end{Bmatrix}, \quad \{\mathbf{Q}\} = \begin{Bmatrix} Q_{ai} \\ Q_{bi} \end{Bmatrix},$$

ΔF and $\Delta\Omega$ represent increments in the amplitude and frequency of excitation, respectively K_{ij}^{cc}, K_{ij}^{cs}, K_{ij}^{sc}, K_{ij}^{ss} refer to the elements of the Jacobian matrix and R_{ai} and R_{bi} are the components of the residue vector.

The form of the Jacobian for linear terms as well as cubic stiffness have been derived in reference [3]. In the present paper, explicit formulae for the Jacobian matrix and residue vector as applicable to the form of damping in equation (2) is derived. The same results can also be used for other forms of damping given in equation (1) for $p \leqslant 3$. Consider the piecewise non-linear damping force to be of the form

$$f(\dot{x}) = \begin{cases} \alpha_1\dot{x}^3 + \alpha_2\dot{x}^2 + \alpha_3\dot{x} + \alpha_4 & \text{if } \dot{x} > b \\ 0 & \text{if } -b \leqslant \dot{x} \leqslant b. \\ \alpha_5\dot{x}^3 + \alpha_6\dot{x}^2 + \alpha_7\dot{x} + \alpha_8 & \text{if } \dot{x} < -b \end{cases} \tag{9}$$

The non-linearity in equation (2) with the use of equation (3) can be expressed in equation (9) with appropriate values for the α_is and with $b = 0$. It is therefore clear that one needs to obtain the zeros of the above equation. In the computer simulation this is achieved at each iteration through a procedure which uses bisection and interpolation methods on the velocity vector similar to the method adopted in reference [4] for the displacement vector. The knowledge of the vector products is also essential for evaluating the Jacobian matrix and residue vector. The Fourier series for products of velocity vectors are derived in the sequel.

3.2. *Fourier series for product of velocity vectors*

The double product of the velocity vectors can be expressed as

$$\{\dot{x}(\tau)\dot{x}(\tau)\} = \dot{A}_o + \sum_{k=1}^{2N} \dot{A}_k^c \cos k\tau + \dot{A}_k^s \sin k\tau. \tag{10}$$

The $\dot{A}_o$, $\dot{A}_k^c$ and $\dot{A}_k^s$ are given by

$$\dot{A}_o = \frac{1}{2}\sum_{i=1}^{N} i^2 A_o,$$

$$\dot{A}_k^c = \dot{A}_{k1}^c + \dot{A}_{k2}^c + \dot{A}_{k3}^c,$$

$$\dot{A}_k^s = \dot{A}_{k1}^s + \dot{A}_{k2}^s + \dot{A}_{k3}^s,$$

where

$$\dot{A}_{k1}^c = \dot{A}_{k1}^s = 0,$$

$$\dot{A}_{k2}^c = \begin{cases} (i+k)iA_{k2}^c & \text{if } (i+k) \leqslant N \\ 0 & \text{otherwise} \end{cases},$$

$$\dot{A}^s_{k2} = \begin{cases} (i+k)iA^s_{k2} & \text{if } (i+k) \leqslant N \\ 0 & \text{otherwise} \end{cases},$$

$$\dot{A}^c_{k3} = \begin{cases} (i-k)iA^c_{k3} & \text{if } |i-k| \leqslant N \text{ and } |i-k| \geqslant 1 \\ 0 & \text{otherwise} \end{cases},$$

$$\dot{A}^s_{k3} = \begin{cases} (i-k)iA^s_{k3} & \text{if } |i-k| \leqslant N \text{ and } |i-k| \geqslant 1 \\ 0 & \text{otherwise} \end{cases}.$$

Expressions for A^c_{k2}, A^s_{k2}, A^c_{k3}, A^s_{k3} are given in terms of the Fourier coefficients a_is and b_is as

$$A^c_{k2} = \begin{cases} 1/2 \sum_{i=1}^{N} a_{i+k}a_i + 1/2 \sum_{i=1}^{N} b_{i+k}b_i & \text{if } (i+k) \leqslant N \\ 0 & \text{otherwise} \end{cases},$$

$$A^s_{k2} = \begin{cases} 1/2 \sum_{i=1}^{N} b_{i+k}a_i + 1/2 \sum_{i=1}^{N} - a_{i+k}b_i & \text{if } (i+k) \leqslant N \\ 0 & \text{otherwise} \end{cases},$$

$$A^c_{k3} = \begin{cases} 1/2 \sum_{i=1}^{N} a_{|i-k|}a_i + 1/2 \sum_{i=1}^{N} \operatorname{sgn}(i-k) b_{|i-k|}b_i & \text{if } |i-k| \leqslant N \text{ and } |i-k| \geqslant 1 \\ 0 & \text{otherwise} \end{cases},$$

$$A^s_{k3} = \begin{cases} 1/2 \sum_{i=1}^{N} \operatorname{sgn}(k-i) b_{|i-k|}a_i + 1/2 \sum_{i=1}^{N} \operatorname{sgn}^2(k-i) a_{|i-k|}b_i \\ 0 \end{cases}$$

$$\begin{matrix} \text{if } |i-k| \leqslant N \text{ and } |i-k| \geqslant 1 \\ \text{otherwise} \end{matrix}.$$

Likewise, the triple product of the velocity vectors can be expressed as follows:

$$\{\dot{x}(\tau)\dot{x}(\tau)\dot{x}(\tau)\} = \dot{B}_o + \sum_{k=1}^{3N} (\dot{B}^c_k \cos k\tau + \dot{B}^s_k \sin k\tau). \tag{11}$$

The $\dot{B}_o$, $\dot{B}^c_k$ and $\dot{B}^s_k$ are given by

$$\dot{B}_o = 1/2 \sum_{i=1}^{N} (i\dot{A}^c_i b_i - i\dot{A}^s_i a_i),$$

$$\dot{B}^c_k = \dot{B}^c_{k1} + \dot{B}^c_{k2} + \dot{B}^c_{k3},$$

$$\dot{B}^s_k = \dot{B}^s_{k1} + \dot{B}^s_{k2} + \dot{B}^s_{k3},$$

where

$$\dot{B}^c_{k1} = \begin{cases} k\dot{A}_o b_k & \text{if } k \leqslant N \\ 0 & \text{otherwise} \end{cases},$$

$$\dot{B}^s_{k1} = \begin{cases} -k\dot{A}_o a_k & \text{if } k \leqslant N \\ 0 & \text{otherwise} \end{cases},$$

$$\dot{B}^c_{k2} = \begin{cases} 1/2 \sum_{i=1}^{N} (i\dot{A}^c_{i+k} b_i - i\dot{A}^s_{i+k} a_i) & \text{if } (i+k) \leqslant 2N \\ 0 & \text{otherwise} \end{cases},$$

$$\dot{B}^s_{k2} = \begin{cases} 1/2 \sum_{i=1}^{N} (i\dot{A}^s_{i+k} b_i + i\dot{A}^c_{i+k} a_i) & \text{if } (i+k) \leqslant 2N \\ 0 & \text{otherwise} \end{cases},$$

$$\dot{B}^c_{k3} = \begin{cases} 1/2 \sum_{i=1}^{N} i\dot{A}^c_{|i-k|} b_i - i \operatorname{sgn}(i-k)\dot{A}^s_{|i-k|} a_i & \text{if } |i-k| \leqslant 2N \text{ and } |i-k| \geqslant 1 \\ 0 & \text{otherwise} \end{cases},$$

$$\dot{B}^s_{k3} = \begin{cases} 1/2 \sum_{i=1}^{N} (i \operatorname{sgn}(k-i)\dot{A}^s_{|i-k|} b_i - i\dot{A}^c_{|i-k|} a_i) & \text{if } |i-k| \leqslant 2N \text{ and } |i-k| \geqslant 1 \\ 0 & \text{otherwise} \end{cases}.$$

3.3. *Residue vector and Jacobian for general damping*

The elements of the Jacobian matrix and residue vector are derived in closed form for a general piecewise non-linear damping as given in equation (9) in the following form:

$$\begin{aligned} R_{ai} = H\Bigg[\sum_{l=0}^{L} \Bigg\{ & \sum_{k=0}^{3N} \beta_1 \{ \dot{B}^c_k [A_{ik}(\theta_{l+1}) - A_{ik}(\theta_l)] + \dot{B}^s_k [B_{ik}(\theta_{l+1}) - B_{ik}(\theta_l)] \} \\ & + \sum_{k=0}^{2N} \beta_2 \{ \dot{A}^c_k [A_{ik}(\theta_{l+1}) - A_{ik}(\theta_l)] + \dot{A}^s_k [B_{ik}(\theta_{l+1}) - B_{ik}(\theta_l)] \} \\ & + \sum_{k=0}^{N} \beta_3 \{ c_k [A_{ik}(\theta_{l+1}) - A_{ik}(\theta_l)] + d_k [B_{ik}(\theta_{l+1}) - B_{ik}(\theta_l)] \} \\ & + \beta_4 [E_i(\theta_{l+1}) - E_i(\theta_l)] \Bigg\} \Bigg], \end{aligned} \tag{12}$$

$$\begin{aligned} R_{bi} = H\Bigg[\sum_{l=0}^{L} \Bigg\{ & \sum_{k=0}^{3N} \beta_1 \{ \dot{B}^c_k [C_{ik}(\theta_{l+1}) - C_{ik}(\theta_l)] + \dot{B}^s_k [D_{ik}(\theta_{l+1}) - D_{ik}(\theta_l)] \} \\ & + \sum_{k=0}^{2N} \beta_2 \{ \dot{A}^c_k [C_{ik}(\theta_{l+1}) - C_{ik}(\theta_l)] + \dot{A}^s_k [D_{ik}(\theta_{l+1}) - D_{ik}(\theta_l)] \} \\ & + \sum_{k=0}^{N} \beta_3 \{ c_k [C_{ik}(\theta_{l+1}) - C_{ik}(\theta_l)] + d_k [D_{ik}(\theta_{l+1}) - D_{ik}(\theta_l)] \} \\ & + \beta_4 [F_i(\theta_{l+1}) - F_i(\theta_l)] \Bigg\} \Bigg], \end{aligned} \tag{13}$$

$$K_{ij}^{cc} = -\frac{j}{2} H\Bigg[\sum_{l=0}^{L}\Bigg\{\sum_{k=0}^{2N}\beta_1[\dot{A}_k^c(B_{k,i+j}(\theta_{l+1}) - B_{k,i+j}(\theta_l)) + \operatorname{sgn}(j-i)(B_{k,|i-j|}(\theta_{l+1})$$

$$- B_{k,|i-j|}(\theta_l)) + \dot{A}_k^s(D_{k,i+j}(\theta_{l+1}) - D_{k,i+j}(\theta_l)) + \operatorname{sgn}(j-i)(D_{k,|i-j|}(\theta_{l+1})$$

$$- D_{k,|i-j|}(\theta_l))] + \sum_{k=0}^{N}\beta_2[c_k(B_{k,i+j}(\theta_{l+1}) - B_{k,i+j}(\theta_l)) + \operatorname{sgn}(j-i)(B_{k,|i-j|}(\theta_{l+1})$$

$$- B_{k,|i-j|}(\theta_l)) + d_k(D_{k,i+j}(\theta_{l+1}) - D_{k,i+j}(\theta_l)) + \operatorname{sgn}(j-i)(D_{k,|i-j|}(\theta_{l+1})$$

$$- D_{k,|i-j|}(\theta_l))] + \beta_3(B_{ij}(\theta_{l+1}) - B_{ij}(\theta_l))\Bigg\}\Bigg], \tag{14}$$

$$K_{ij}^{cs} = \frac{j}{2} H\Bigg[\sum_{l=0}^{L}\Bigg\{\sum_{k=0}^{2N}\beta_1[\dot{A}_k^c(A_{k,i+j}(\theta_{l+1}) - A_{k,i+j}(\theta_l)) + (A_{k,|i-j|}(\theta_{l+1}) - A_{k,|i-j|}(\theta_l))$$

$$+ \dot{A}_k^s(C_{k,i+j}(\theta_{l+1}) - C_{k,i+j}(\theta_l)) + (C_{k,|i-j|}(\theta_{l+1}) - C_{k,|i-j|}(\theta_l))]$$

$$+ \sum_{k=0}^{N}\beta_2[c_k(A_{k,i+j}(\theta_{l+1}) - A_{k,i+j}(\theta_l)) + (A_{k,|i-j|}(\theta_{l+1}) - A_{k,|i-j|}(\theta_l))$$

$$+ d_k(C_{k,i+j}(\theta_{l+1}) - C_{k,i+j}(\theta_l)) + (C_{k,|i-j|}(\theta_{l+1}) - C_{k,|i-j|}(\theta_l))]$$

$$+ \beta_3(A_{ij}(\theta_{l+1}) - A_{ij}(\theta_l))\Bigg\}\Bigg], \tag{15}$$

$$K_{ij}^{sc} = -\frac{j}{2} H\Bigg[\sum_{l=0}^{L}\Bigg\{\sum_{k=0}^{2N}\beta_1[\dot{A}_k^c\{(-A_{k,i+j}(\theta_{l+1}) + A_{k,i+j}(\theta_l)) + (A_{k,|i-j|}(\theta_{l+1}) - A_{k,|i-j|}(\theta_l))\}$$

$$+ \dot{A}_k^s\{(-C_{k,i+j}(\theta_{l+1}) + C_{k,i+j}(\theta_l)) + (C_{k,|i-j|}(\theta_{l+1}) - C_{k,|i-j|}(\theta_l))\}]$$

$$+ \sum_{k=0}^{N}\beta_2[c_k\{(-A_{k,i+j}(\theta_{l+1}) + A_{k,i+j}(\theta_l)) + (A_{k,|i-j|}(\theta_{l+1}) - A_{k,|i-j|}(\theta_l))\}$$

$$+ d_k\{(-C_{k,i+j}(\theta_{l+1}) + C_{k,i+j}(\theta_l)) + (C_{k,|i-j|}(\theta_{l+1}) - C_{k,|i-j|}(\theta_l))\}]$$

$$+ \beta_3(D_{ij}(\theta_{l+1}) - D_{ij}(\theta_l))\Bigg\}\Bigg], \tag{16}$$

$$K_{ij}^{ss} = -K_{ji}^{cc}, \tag{17}$$

where H is the Heaveside unit step function, and $\beta_i = \alpha_i$ if $\dot{x} > b$ and $\beta_i = \alpha_i + 4$ if $\dot{x} < -b$, $i = 1, \ldots 4$.

In the above equations L represents the number of zeros of the velocity vector. Also $c_k = kb_k^s$, $d_k = -ka_k^c$ and the expressions for A, B, C, D, E and F are given by

$$A_{m,n}(\theta_l) = \theta_l\left[\frac{\sin(m-n)\theta_l}{(m-n)\theta_l} + \frac{\sin(m+n)\theta_l}{(m+n)\theta_l}\right],$$

$$B_{m,n}(\theta_l) = \begin{cases} \theta_l\left[\dfrac{\cos(m-n)\theta_l}{(m-n)\theta_l} - \dfrac{\cos(m+n)\theta_l}{(m+n)\theta_l}\right] & \text{if } m \neq n \\ -\theta_l\left[\dfrac{\cos(2m\theta_l)}{(2m\theta_l)}\right] & \text{if } m = n \end{cases},$$

$$C_{m,n}(\theta_l) = B_{n,m}(\theta_l),$$

$$D_{m,n}(\theta_l) = \theta_l\left[\frac{\sin(m-n)\theta_l}{(m-n)\theta_l} + \frac{\sin(m+n)\theta_l}{(m+n)\theta_l}\right],$$

$$E_m(\theta_l) = \theta_l\left[\frac{\sin m\theta_l}{m\theta_l}\right],$$

$$F_m(\theta_l) = -\theta_l\left[\frac{\cos m\theta_l}{m\theta_l}\right].$$

4. BIFURCATION AND STABILITY ANALYSIS

One can obtain both stable and unstable periodic solutions of the dynamical system by the use of the IHB method, unlike the numerical integration method which gives only stable solutions. Hence, the stability of the solutions obtained by the IHB method must be determined to know whether such a solution is possible in reality. The stability of the periodic solutions is investigated by perturbing the state variables about the steady state solutions. The monodromy matrix or transition matrix relating the states of the system at the beginning and at the end of one period of motion is determined by using the approximate procedure given by Friedmann *et al*. [7]. The eigenvalues of the monodromy matrix are the Floquet multipliers corresponding to the periodic solution. The periodic solution would be stable if all the eigenvalues of the monodromy matrix lie within the unit circle. As a system parameter is varied the eigenvalues also move and if any one of the eigenvalues crosses the unit circle the corresponding periodic solution loses stability leading to another type of solution. The way in which the eigenvalue crosses the unit circle indicates the nature of bifurcation. In this paper the periodic solutions and the nature of bifurcations as a system parameter is varied are obtained by a parameter continuation and path following method [6].

5. RESULTS AND DISCUSSION

The periodic motions of the non-linear oscillator of equation (2) is investigated by the IHB method in conjunction with the stability analysis and path following procedure. F is taken as the bifurcation parameter in the range 0·2–7. The values of ξ and Ω are taken as 0·025 and 1·0, respectively. The maximum amplitude of the different periodic responses are plotted as a function of the bifurcation F and the response (bifurcation) diagram is

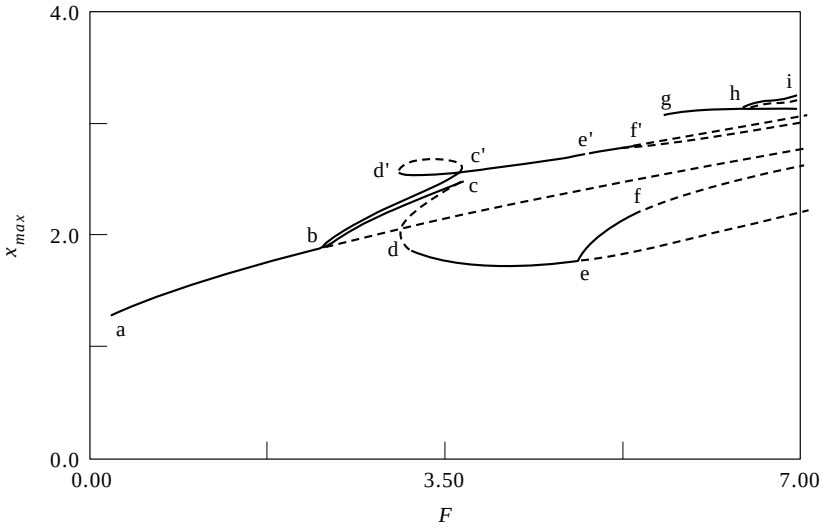

Figure 1. Response diagram, $\xi = 0{\cdot}025$, $\Omega = 1{\cdot}0$.

shown in Figure 1. The stable branches are represented by full lines and the unstable branches by dotted lines.

Starting from point a ($F = 0{\cdot}2$) the system exhibits a symmetric period 1 motion until the point b ($F = 2{\cdot}2487$). At this point, the symmetric solution becomes unstable and bifurcates to an asymmetric solution through a symmetry breaking bifurcation which is

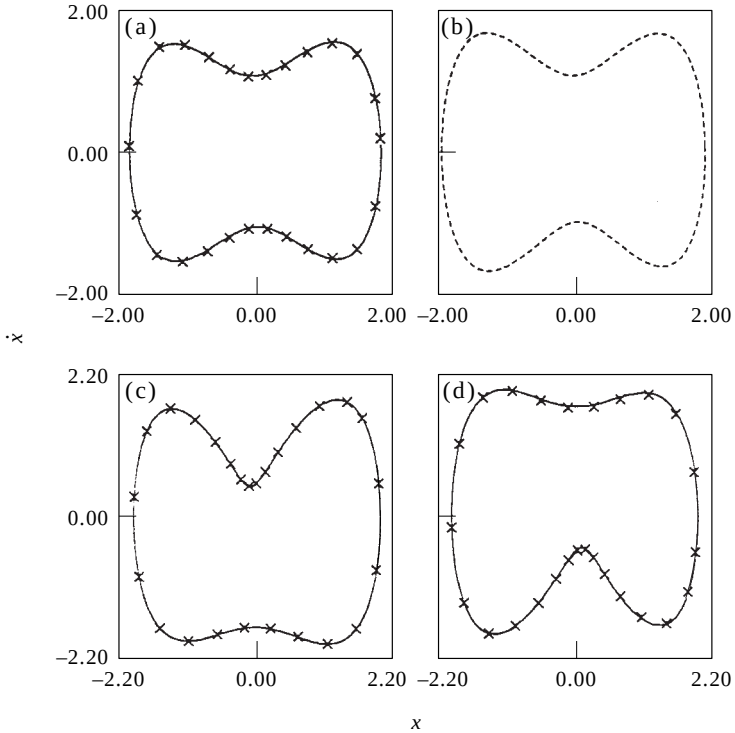

Figure 2. Phase plane of period 1 responses, $\xi = 0{\cdot}025$, $\Omega = 1{\cdot}0$: (a) $F = 2{\cdot}0$, stable symmetric period 1; (b) $F = 2{\cdot}40$, unstable symmetric period 1; (c, d) $F = 2{\cdot}40$, dual unsymmetric period 1.

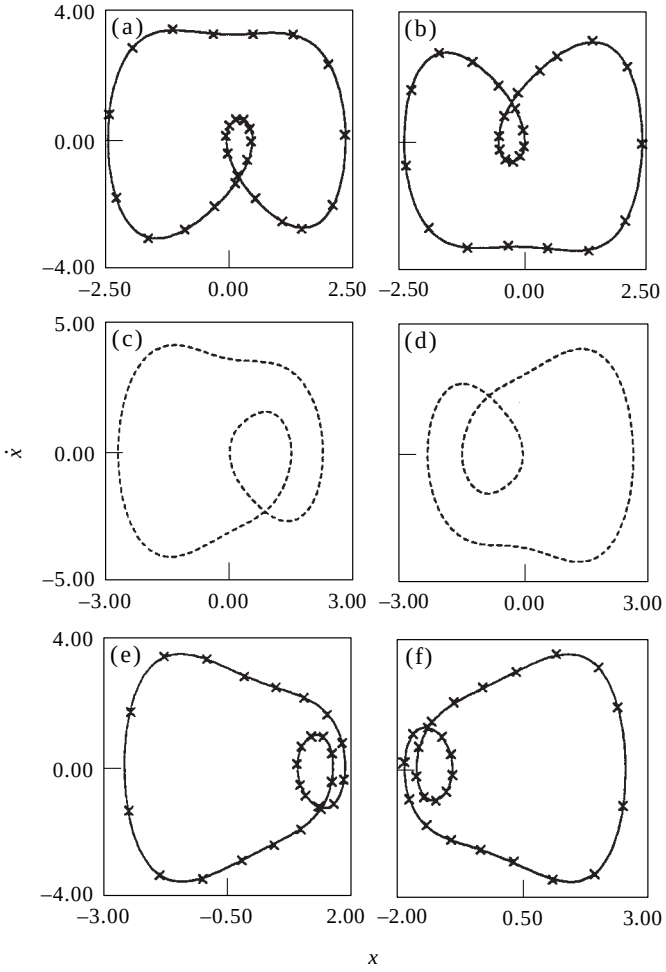

Figure 3. Phase plane of multiple period 1 responses, $\xi = 0{\cdot}025$, $\Omega = 1{\cdot}0$, $F = 3{\cdot}3$: (a) path b–c; (b) path b–c′; (c) path c–d; (d) path c′–d′; (e) path d–e; (f) path d′–e′.

confirmed from noting that the eigenvalue of the monodromy matrix takes a value of $+1$ at point b. The phase plane of the stable period 1 symmetric solution at $F = 2{\cdot}0$ is shown in Figure 2(a). The unstable period 1 symmetric solution and the dual period 1 solutions corresponding to $F = 2{\cdot}4$ obtained by the IHB method are given in Figures 2(b)–(d). The solutions obtained by numerical integration are superposed in Figures 2(a), (c) and (d) by the crosses which show the close fit between the solutions obtained by the IHB method and numerical integration.

On a further increase in F the dual periodic solutions continue to exist as seen by the two stable branches (bc, bc′) in the response diagram. At points c and c′ ($F = 3{\cdot}683$) a saddle node bifurcation occurs which is concluded from noting that the sets of Floquet multipliers move out of the unit circle along the $+1$ direction. The unstable dual period 1 solutions are traced back by the path following algorithm shown by the dotted branches cd and c′d′. The points d and d′ correspond to $F = 3{\cdot}076$ at which the Floquet multipliers enter the unit circle in the -1 direction resulting in stable period 1 solutions represented by the solution branches de and d′e′. Thus, between the regions c and d (c′ and d′), four stable period 1 solutions and two unstable period 1 solutions are exhibited. The phase

diagrams of the stable and unstable multiple solutions corresponding to $F = 3{\cdot}3$ obtained by the IHB method are shown in Figures 3(a)–(f). As before, the stable solutions obtained by numerical integration are superposed by the crosses, which once again shows the excellent fit obtained by the IHB method. In computing and tracing these period 1 solutions, eight harmonics were used in the finite Fourier series in the IHB method.

With a further increase in F the dual period 1 solutions undergo period doubling bifurcations at e and e′ ($F = 4{\cdot}844$). This is confirmed by the movement of the Floquet multipliers out of the unit circle along the -1 direction at these two points. These dual period 2 solutions further bifurcate into period 4 solutions at f and f′ ($F = 5{\cdot}32$). These period 4 solutions further undergo a series of period doubling bifurcations resulting in chaotic response. These dual subharmonic responses of order 2, 4 and 8 obtained by the IHB method are shown in Figures 4(a)–(f). The numerical integration results are also shown by crosses showing the excellent fit between the two. The number of harmonics used are 24, 32, 64, respectively, for period 2, period 4 and period 8 responses.

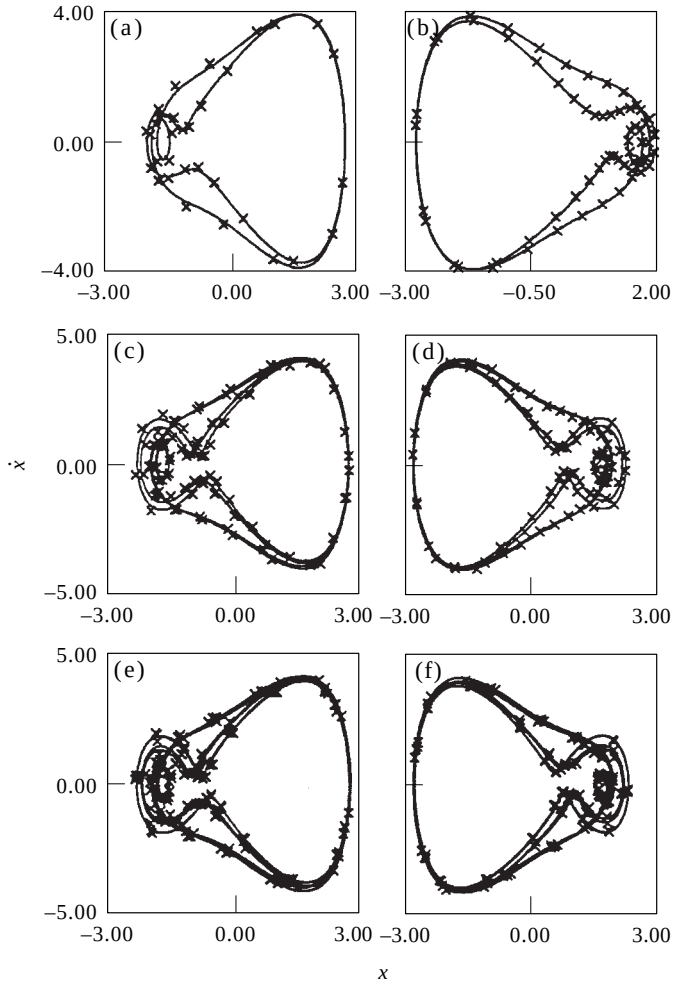

Figure 4. Phase plane of subharmonic responses, $\xi = 0{\cdot}025$, $\Omega = 1{\cdot}0$: (a, b) $F = 5{\cdot}0$, dual period 2; (c, d) $F = 5{\cdot}3$, dual period 4; (e, f) $F = 5{\cdot}45$, dual period 8.

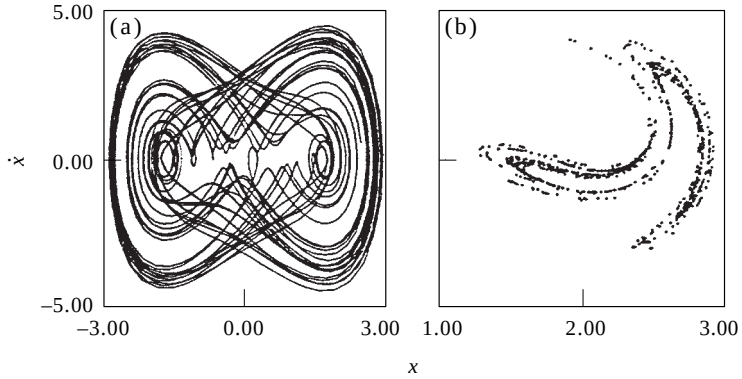

Figure 5. Chaotic response, $\xi = 0{\cdot}025$, $\Omega = 1{\cdot}0$, $F = 5{\cdot}6$: (a) phase plane; (b) Poincare' section.

The chaotic motion exists over a narrow range of F and Figures 5(a) and (b) give the phase plane diagram and Poincare' section of the chaotic motion at $F = 5{\cdot}60$. The unclosed phase plane and fractal nature of the Poincare' section qualitatively indicate chaotic motion, which is quantitatively confirmed by computing the Lyapunov exponents. One of the Lyapunov exponents is positive in this region and at $F = 5{\cdot}6$ the positive Lyapunov exponent has a value (0·18544). The chaotic regions cannot be shown in the response diagram of Figure 1 as it is entirely obtained by the IHB method while the chaotic solutions are obtained only by numerical integration.

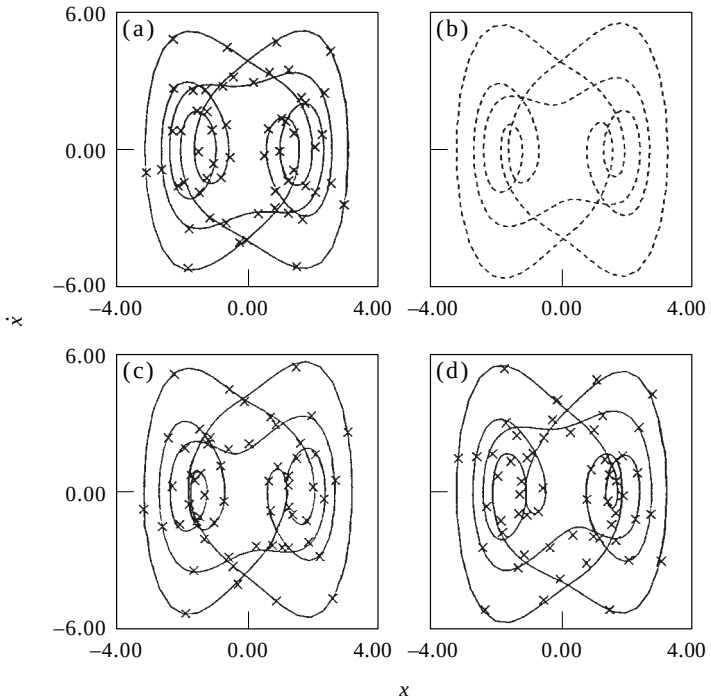

Figure 6. Period 3 responses, $\xi = 0{\cdot}025$, $\Omega = 1{\cdot}0$: (a) $F = 5{\cdot}80$, stable symmetric period 3; (b) $F = 6{\cdot}6$, unstable symmetric period 3; (c, d) $F = 6{\cdot}6$, dual unsymmetric period 3.

On a further increase in F a remote symmetric period 3 motion appears at point g ($F = 5{\cdot}70$). At point h ($F = 6{\cdot}45$), it loses stability through symmetric breaking bifurcation resulting in dual unsymmetric period 3 motions. These dual period 3 motions undergo period doubling bifurcations at i ($F = 6{\cdot}92$) resulting in dual period 6 motions. The phase plane diagrams of stable symmetric period 3, unstable symmetric period 3 and dual unsymmetric period 3 responses obtained by the IHB method are given in Figure 6. Once again the comparisons between the numerically integrated solutions and IHB solutions of the stable period 3 solutions are very good. In IHB solutions, 45 harmonics were used in the finite Fourier series for obtaining these period 3 solutions. It was found by numerical integration that the period 6 solutions undergo further period doubling leading to chaos.

6. SUMMARY AND CONCLUSIONS

The IHB method is used to obtain the periodic responses of a non-linear oscillator with an orifice type of damping and cubic stiffness. Closed form expressions are derived for the elements of the Jacobian matrix and other derivative vectors for different types of general non-linear damping mechanisms. These are applied to the specific cases of the orifice damping. The results obtained by the IHB method match very well with those obtained by numerical integration showing the efficacy of the method to treat piecewise non-linear damping mechanisms. The IHB method can also be combined effectively with stability analysis and parameter continuation to trace the bifurcations of the non-linear system as is demonstrated by the problem considered. For the non-linear system with orifice damping, different types of bifurcations such as symmetry breaking, saddle node and period doubling are found to occur. Multiple periodic responses exist for the same system parameters. The period doubling cascade leading to chaos is investigated by numerical integration. Period 3 subharmonic responses also exist in certain ranges of F as is the case with many non-linear systems with cubic stiffness. The period 3 responses are also accurately obtained by the IHB method.

REFERENCES

1. B. Ravindra and A. K. Mallik 1995 *Journal of Sound and Vibration* **182**, 345–353. Chaotic response of a harmonically excited mass on an isolator with nonlinear stiffness and damping characteristics.
2. S. L. Lau, Y. K. Cheung and S. Y. Wu 1982 *ASME Journal of Applied Mechanics* **49**, 849–853. A variable parameter incremental method for dynamic instability of linear and nonlinear elastic systems.
3. A. Y. T. Leung and T. C. Fung 1989 *Journal of Sound and Vibration* **131**, 445–455. Construction of chaotic regions.
4. S. L. Lau and W. S. Zhang 1992 *ASME Journal of Applied Mechanics* **59**, 153–160. Nonlinear vibrations of piecewise linear systems by incremental harmonic balance method.
5. C. Pierre, A. A. Ferri and E. H. Dowell 1985 *Transactions of the American Society of Mechanical Engineers*, *Journal of Applied Mechanics* **50**, 958–964. Multi-harmonic analysis of dry friction damped systems using an incremental harmonic balance method.
6. A. Y. T. Leung and S. K. Chui 1995 *Journal of Sound and Vibration* **181**, 619–633. Nonlinear vibration of coupled Duffing oscillators by an improved incremental harmonic balance method.
7. P. Friedmann, C. E. Hammond and T. H. Woo 1977 *International Journal of Numerical Methods in Engineering* **11**, 1117–1136. Efficient numerical treatment of periodic systems with application to stability problems.